INSIGHTS INTO IO'S INTERIOR AS INFERRED FROM ITS LONG-WAVELENGTH TOPOGRAPHY.
S. Gyalay[1] and F. Nimmo[1], [1]University of California, Santa Cruz (sgyalay@ucsc.edu)

Introduction: It is a mystery whether Jupiter's hypervolcanic satellite Io hides a magma ocean beneath its crust [1]. Such an ocean would have implications for the distribution and transport of tidal heating within the moon. Indeed, discerning Io's interior is a primary goal of Io Volcano Observer (IVO), a proposed mission that would perform successive flybys of Io [2]. In recent work [3], we demonstrated the ability to use the observed long-wavelength topography of Saturn's icy satellites to infer the tidal heating distribution below the ice shell, which is a window into its interior structure. We propose to apply a similar methodology to Io to make a prediction on the presence of a magma ocean that can be confirmed by future flybys of Io—be it by IVO or during Juno's extended mission.

The Relationship Between Tidal Heating and Topography: Previous studies have investigated the link between Io's tidal heating and its lithospheric thickness [4, 5], the latter of which can be translated to topography by assuming isostasy. [6] argued that to satisfy the seemingly-paradoxical, observed constraints of mountainous terrain and high surface heat flux, Io must advect much of its heat through a thick, cold lithosphere via heat pipes of magma that erupt upon the surface. [4] incorporated this into their study by using melt production from tidal dissipation to heat the lithosphere and predict surface topography. Our approach differs from theirs in a few key ways.

We make the simplifying assumption that if tidal heating operates at the base of the lithosphere or deeper, it provides a total heat flux F as described by equations (1) and (3b) of [6]:

$$F = v\rho\left[\Delta H_{\mathrm{f}} + \mathrm{C_p}(T_m - T_s)\right] + \frac{vk(T_m - T_s)}{\alpha(e^{vd/\alpha} - 1)}, \quad (1)$$

where v is the resurfacing rate, ρ is the magma density, ΔH_f is the latent heat of fusion, C_p is the specific heat, T_m is the melting temperature, T_s is the surface temperature, k is the lithosphere's thermal conductivity, α the thermal diffusivity, and d the lithospheric thickness.

In contrast to [4], this equation implies the lithosphere thins when tidal dissipation increases (for some given resurfacing/emplacement rate). We also assume that this lithosphere experiences Airy isostasy, rather than Pratt as in [4], and can find the topography h from the change in lithosphere thickness Δd from the average as

$$h = \frac{\Delta d}{1 + (\rho/\Delta\rho)}, \quad (2)$$

where Δρ is the density contrast between the lithosphere and underlying mantle or magma. We do not expect the lithospheric thickness to be significant compared to Io's radius and thus make no correction to account for a spherical geometry [cf. 7]. If a magma ocean is present, we assume that the crust and lithosphere are effectively the same (following [6]) and that they float isostatically atop the magma beneath.

Spatial Patterns of Tidal Heating: When described in spherical harmonics, the distribution of tidal heating across a globe can be described using only coefficients of even order in degrees 2 and 4 [8]. Further, [8] established that a tidal heating distribution $F(\theta,\lambda)$ can be described as the linear combination of three basis heating patterns A, B, and C—themselves combinations of the spherical harmonic coefficients of tidal heating:

$$F(\theta,\lambda) = \frac{F_0}{a_{0,0}}(\chi_A\psi_A + \chi_B\psi_B + \chi_C\psi_C), \quad (3)$$

where F_0 is the average heat flux due to tidal heating, ψ denotes a heating pattern as a function of colatitude θ and longitude λ; and χ is that heating pattern's weight such that the sum of the weights is 1. $a_{l,m}$ is a constant dependent on spherical harmonic degree l and order m, found in [8]. We assume tidal heating on Io is due to eccentricity tides.

One can generate a tidal heating distribution for an assumed average heat flux and heating pattern weights (e.g. for a thin lithosphere, a fluid interior has a high χ_C, while a rigid interior has a high χ_B). If we instead deduce the heat flux distribution from the measured topography using equations (1) and (2) for some assumed average lithospheric thickness and resurfacing rate, we can calculate the best-fit heating pattern weights to our inferred heating pattern [3]. Following the definitions of [8]'s heating patterns, we compose a system of equations relating spherical harmonic coefficients of flux $C^F_{l,m}$ to heating pattern weights:

$$\frac{a_{0,0}}{a_{l,m}}\frac{C^F_{l,m}}{F_0} - 1 = \begin{cases} -\frac{1}{2}\chi_B - 2\chi_C, if\ l = 2, \\ -\frac{5}{3}\chi_B - \frac{5}{6}\chi_C, if\ l = 4. \end{cases} \quad (4)$$

By performing a multi-linear regression, we can calculate the heating pattern weights that best describe our inferred heating distribution, along with the coefficient of determination R^2 of the regression, which in this case describes how well tidal heating describes the topography-derived heat flux distribution (where a maximum of 1 fits best).

Best-Fit Tidal Heating Pattern for Io: We calculate spherical harmonic coefficients of topography for Io from limb profiles [9, 10]. The errors in degree 2 and $C_{4,0}$ topography are one order of magnitude less than the coefficient, while errors in $C_{4,2}$ and $C_{4,4}$ are the same order as the coefficient. The bulk of degree 2 topography is due to rotational flattening and tidal stretching [e.g. 11], dependent on a term related to Io's moment of inertia (MoI) by the Darwin-Radau relation [e.g. 12]. Io's MoI has been found by gravitational measurements [13]. We adopt values for thermal conductivity, specific heat capacity, heat of fusion, thermal diffusivity and melting temperature from [6]; an average surface temperature of 110 K from [14], a crustal density of 3000 kg m^{-3} from [4], and we assume a mantle density of 3300 kg m^{-3}.

We calculate the variation in lithospheric thickness from the observed topography via isostasy using equation (2). As the residual topography (topography less rotational flattening/tidal stretching) varies on the order 0.3 km, the lithospheric thickness variations are on the order 3 km.

We vary two parameters: the average resurfacing rate v_0 and the average lithospheric thickness d_0 (from which one can calculate the average heat flux F_0). Like [4], we assume two endmember cases: resurfacing is either uniform across Io's globe or directly proportional to tidal heating (i.e. $v = v_0 F/F_0$). How well the tidal heating pattern weights approximate the inferred heat flux distribution is plotted in Figure 1.

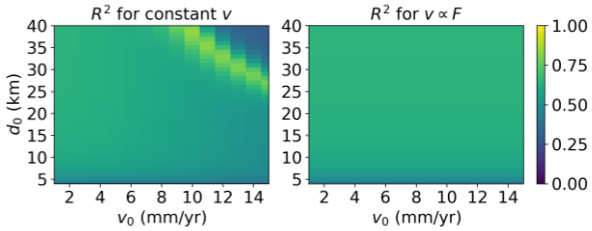

Figure 1: The coefficient of determination R^2 of how well the inferred flux distribution from each combination of parameters can be represented by a tidal heating distribution.

Both cases exhibit a relatively uniform R^2, but a band in the constant v case exhibits a better fit than the other parameter combinations. Along this band (where R^2 peaks at 0.82), the heating pattern weights are exactly what one expects from a uniform flux field, while best-fit heating pattern weights outside the band (and in the $v \propto F$ case) still represent nearly uniform flux fields. In the future, we will examine a case where v varies with volcanic frequency without the requirement of being proportional to F [e.g. 15].

Discussion: Such little variation between best-fit heating patterns across the parameter space could naïvely be blamed on the uncertainty of long-wavelength topography. However, under the thickest lithospheres and highest resurfacing rates, the advective (first) term of the heat flux dominates the conductive (second) term of equation (1), by e.g. six orders of magnitude for $d_0 = 40$ km and $v_0 = 10$ mm yr^{-1}. As only the conductive term relies lithospheric thickness, very small changes in the *total* heat flux are necessary to produce the $l = 2{,}4$ topography on the order of 0.3 km that we observe. We confirm this by calculating forward models of topography (Figure 2): typical predicted relief for the expected tidal variations in heat flux is on the order of a few km, except at the very lowest lithospheric thicknesses. However, at low lithospheric thickness we are unable to find reasonable fits to the observed topography. So, our conclusion of a uniform heat flux appears to be robust.

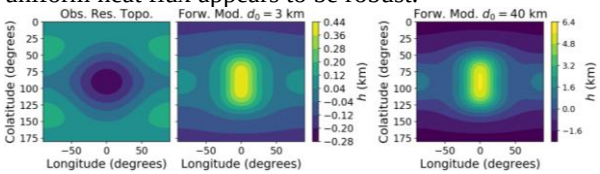

Figure 2: (Left) Observed residual topography of Io. (Middle) Example forward modeled topography for $d_0 = 3$ km, $v_0 = 10$ mm yr^{-1}. (Right) Same as previous but for $d_0 = 40$ km.

Typically, a uniform heat flux would indicate a uniform heat source such as radionuclides, but Io is only as hot as it is *because* of tidal heating. Thus our results suggest that while solid-body tidal heating may produce a unique heat flux distribution [16], something efficiently redistributes heat evenly enough to destroy any spatial variation. While it may be possible for convection in the mantle to do so, it is perhaps more likely that a vigorously convecting, subsurface magma ocean is responsible.

References: [1] de Kleer, K. et al. (2011) https://www.kiss.caltech.edu/final_reports/Tidal_Heating_final_report.pdf. [2] McEwen, A.S. et al. (2019), LPSC 50, Abs. 1316. [3] Gyalay, S. et al. (2019), LPSC 50, Abs. 1715. [4] Spencer, D. et al. (2020), in review, https://arxiv.org/pdf/2008.09022.pdf. [5] Steinke, T. et al. (2020), *Icarus 335*. [6] O'Reilley and Davies (1981), *GRL 8*(4). [7] Hemingway, D. and I. Matsuyama (2017), *GRL 44*(15). [8] Beuthe, M. (2013), *Icarus 223*(1), 308. [9] Thomas, P.C. et al. (1998), *Icarus 135*(1), 175. [10] Nimmo, F. and P.C. Thomas (2004), *AGU Fall Meeting*, Abs. P22B-04. [11] Tricarico, P. (2014), *ApJ 782*(2). [12] Munk, W.H. and G.J.F. MacDonald (1960), *The Rotation of the Earth*. [13] Schubert, G. et al. (2004), *Jupiter*, 281. [14] Rathbun, J.A. et al. (2014), *Icarus 169*(1). [15] Steinke, T. et al. (2020), *JGR: Planets 125*(12). [16] Segatz, M. et al. (1988), *Icarus 75*(2).